Catalysis Letters Vol. 111, Nos. 1–2, October 2006 (© 2006)
DOI: 10.1007/s10562-006-0130-y

Rationalizing the catalytic performance of γ-alumina-supported Co(Ni)–Mo(W) HDS catalysts prepared by urea-matrix combustion synthesis

Sergio L. González-Cortés,[a,b,*] Serbia M. A. Rodulfo-Baechler,[b] Tiancun Xiao,[b] and Malcolm L. H. Green[b]

[a]*Laboratorio de Cinética y Catálisis, Departamento de Química, Facultad de Ciencias, Universidad de Los Andes, Mérida, 5101, Venezuela*
[b]*Wolfson Catalysis Centre, Inorganic Chemistry Laboratory, University of Oxford, South Parks Road, Oxford, OX1 3QR, UK*

Received 26 April 2006; accepted 18 July 2006

A comparative study of the influence of Co (or Ni) promoter loadings and the effect of different sulfurizing agents and sulfurizing temperatures on the structure, morphology and catalytic performance of Mo- or W-based hydrodesulfurization (HDS) catalysts was carried out. Catalyst performance using a tubular fixed-bed reactor and the HDS of thiophene as a model reaction was evaluated. The oxidic and sulfurized states of the HDS catalysts were characterized by laser Raman spectroscopy, thermogravimetric analysis (TGA), differential scanning calorimetry (DSC) and high resolution transmission electron microscopy (HRTEM). It has been found that the urea-matrix combustion (UMxC) synthesis is a simple tool for preparing supported catalysts in a short period of thermal treatment. Several consecutive stages such as urea melting, metal precursor dissolution and chemical reactions take place before and upon combustion process. The C_4H_4S/H_2-activated Co- (or Ni-) promoted MoS_2 (or WS_2) catalysts present a strong synergistic effect (SE) when the Co (or Ni)/Mo (or W) molar ratio is near to 0.5, whereas the $C_4/C_4^=$ molar ratios display a weak antagonistic effect. Alumina-supported Ni–W catalyst showed an optimal SE 2.5 times higher than those for Co (or Ni)-promoted Mo HDS catalysts. The kinetic parameters for thiophene-HDS reaction were also determined, suggesting that the C–S bond cleavage reaction for alumina-supported Co(Ni)–Mo HDS catalysts and H_2 activation reaction for Ni-promoted WS_2catalysts play an important role in the rate-limiting step.

KEY WORDS: HDS catalysts; Ni-promoted WS_2 catalysts; Co(Ni)-promoted MoS_2 catalysts; urea-matrix combustion synthesis.

1. Introduction

The stringent environmental regulations in the US, Japan and Europe are requiring significant improvement in the quality of transportation fuel. It is directed toward reducing the amount of sulfur organic compounds in gasoline and diesel fuel to 10 ppm by 2009 [1]. Indeed, zero-emission levels and consequently zero or ultra low sulfur content are called for most of the developed countries in coming 10 years. In order to meet this requirement new catalytic processes or new strategies to improve the hydrodesulfurization (HDS) traditional catalysts (i.e., alumina-supported Co or Ni-promoted Mo or W) are required.

The impregnation methods (i.e., simultaneous or sequential) are the traditional tools for preparing Co(Ni)–Mo and Ni–W HDS catalyst precursors. Normally, ammonium heptamolybdate or ammonium *meta*-tungstate and Co or Ni nitrates are deposited onto γ-alumina at room temperature. After a drying step, the sample is calcined to produce the oxidic precursor and subsequently treated with a mixture of H_2S–H_2 or thiophene and H_2 or using liquid feed of sulfur-containing molecules and H_2 to obtain the sulfurized catalyst [2–4]. Another method that has been successfully applied on the synthesis of HDS catalyst is the chelating method, which consists of incorporating a chelating ligand (e.g., ethylenediamine, nitrilotriacetic acid, ethylenediaminetetraacetic acid) into the impregnating solution in order to complex the metal precursor and hence control its interaction both with the porous support and with the others components of the catalyst [5–7].

Although, the alternative preparation methods have been able to produce advanced HDS catalyst systems [8–11], they require expensive materials or the preparation time is too long or elaborate to be acceptable because of cost. To overcome this drawback, Green and co-workers recently introduced a novel method called urea-matrix combustion (UMxC) for the preparation not only of Co- or Ni-promoted alumina-supported MoS_2 HDS catalysts [12,13], but also of well-dispersed bimetallic and trimetallic molybdate phases on alumina (i.e. model catalysts) [14]. However, a comparative study of the influence of UMCx synthesis on the catalytic behavior of Co(Ni)–Mo(W) HDS catalysts has not been reported yet. Combustion synthesis, based on a self-propagating combustion reaction [15], requires a low

*To whom correspondence should be addressed.
E-mail: goncor@ula.ve

ignition temperature to induce a combustion reaction between the catalyst precursor salts and an organic matrix as fuel (e.g. urea). The final products of combustion might contain a high concentration of structural defects, which are beneficial as active centers in catalysis [16] or catalyst precursors.

Therefore, in the present study an effort is made to rationalize the effect of the UMxC synthesis on the HDS catalytic behavior of alumina-supported Co(Ni)–Mo and Ni–W catalysts. In order to reach this aim not only the influence of different promoter loadings, but also the effect of different sulfurizing agents and sulfurizing temperatures on the structure, morphology and HDS catalytic performance were investigated.

2. Experimental

Bimetallic Co(Ni)–Mo or Ni–W catalyst precursors with 12 wt% MoO_3 or 19 wt% WO_3 and variable wt% CoO (or NiO) loadings supported on γ-Al_2O_3 (164 m^2/g) (Aldrich) were prepared by mixing urea (99%, Aldrich) with ammonium heptamolybdate-4-hydrate (99%, Riedel-de Haën) or ammonium *meta*-tungstate (Fluka) and Co(II) or Ni(II) nitrate (99%, BDH Chemicals). An urea/[W(Mo) + Co(Ni)] molar ratio of 10 and ca. 1 g/2 mL = [Co(or Ni)- and Mo(or W)-precursors + urea]/water ratio were employed. The mixture was stirred to form homogeneous slurry and then mixed with the γ-Al_2O_3 support at ca. 50 °C for 2–3 h to obtain urea-based slurry fully loaded over the alumina. The resulting paste was ignited at 500 °C (furnace temperature) in static air for 10 min to produce the catalyst-oxide precursor.

Two distinct activation processes were employed: (1) Sulfurization using flowing hydrogen saturated with thiophene vapor (ca. 11 mol.% C_4H_4S/H_2) up to 450 °C for 10 h (C_4H_4S pre-sulfided samples). After this process, the catalysts were pretrated with H_2 flowing at 450 °C for 1 h and then they were cooled down to the reaction temperature. (2) Sulfurization employing a gas mixture of 10 mol% H_2S/H_2 up to either 400 °C or 450 °C for 4 h (H_2S pre-sulfided samples). The HDS reactions free of mass transport interference were carried out in a fixed-bed tubular quartz reactor (34 cm long, 4 mm i.d.). Oxidic catalyst precursors (200 mg, < 250 μm) were loaded between quartz wool plugs. The catalysts were tested at atmospheric pressure (0.1 MPa) and the reactants consisted of a 20 $mL.min^{-1}$ H_2 flow saturated with thiophene vapor at 0 °C (2.96 kPa), resulting in a mixture of ca. 3 mol.% thiophene in H_2. The reaction products were analyzed using an on-line HP 5890 Series II chromatograph equipped with a Hayesep R packed column and a flame ionization detector (FID). After completion of the catalytic reaction, the catalyst sample was cooled down to room temperature under flowing argon and then passivated before exposure to the atmosphere and kept in a desiccator thereupon.

The analysis of carbon was carried out using a Vario EL elemental analyzer. The samples were digested through oxidative combustion and the gases analyzed with a thermal conductivity detector.

Thermogravimetric analysis (TGA) and differential scanning calorimetry (DSC) were simultaneously carried out on a Rheometric Scientific STA 1500 instrument. TGA–DSC profiles were recorded from room temperature to 750 °C, using 30 $mL.min^{-1}$ dry air flow and 10 $°C.min^{-1}$ heating rate. For each analysis ca. 25–35 mg of sample was loaded into a small alumina crucible, using alumina as reference.

The Raman spectra of the oxidic precursors and the sulfurized catalysts were recorded in a Jobin Yvon Labram spectrometer with a 632 nm HeNe laser, run in a back-scattered co-focal arrangement. The samples were pressed in a microscope slide; with a 45 s scanning time and 2 cm^{-1} resolution. Several points of each catalyst surface were probed to explore homogeneity of the sample and reproducibility of the data.

High resolution transmission electron microscopy (HRTEM) was carried out using a JEOL 4000FX electron microscope with a 400 kV accelerating voltage. Co(Ni)–Mo sulfurized catalyst was ground into a fine powder and dispersed in AR-grade chloroform. Then, it was placed in an ultrasonic bath for ca. 15 min, before a drop of the suspension was put on a lacey carbon-coated copper grid (Agar, 20 mesh) and subsequently analyzed.

3. Results and discussion

3.1. Characterization of the alumina-supported Co(Ni)–Mo(W) HDS catalysts

3.1.1. Thermal gravimetric analysis (TGA) and differential scanning calorimetry (DSC)

The TGA–DSC profiles in air flowing for the bimetallic alumina-supported 2.5% CoO-12% MoO_3 catalyst precursor are given in Figure 1A. The thermogram shows a weak broad stage at about 85 and a major broad step centered at 191 °C. The first weigh loss is assigned to the desorption of physically adsorbed water molecules on alumina surface [17,18] and the second weight loss is attributed to a complex series of overlapping chemical reactions, such as the partial dehydration–decomposition and the subsequent combustion of the Co and Mo precursor salts and the partial dehydroxylation of alumina [19]. A total weight loss of 46.0 wt%, in correspondence with the expected value (i.e., 45 wt%) assuming the formation of cobalt and molybdenum oxides, was obtained. This indicates that both the urea and the precursor salts are completely decomposed upon the thermal treatment.

On the other hand, the DSC profile displays a weak process at ca. 95 °C associated with desorption of water.

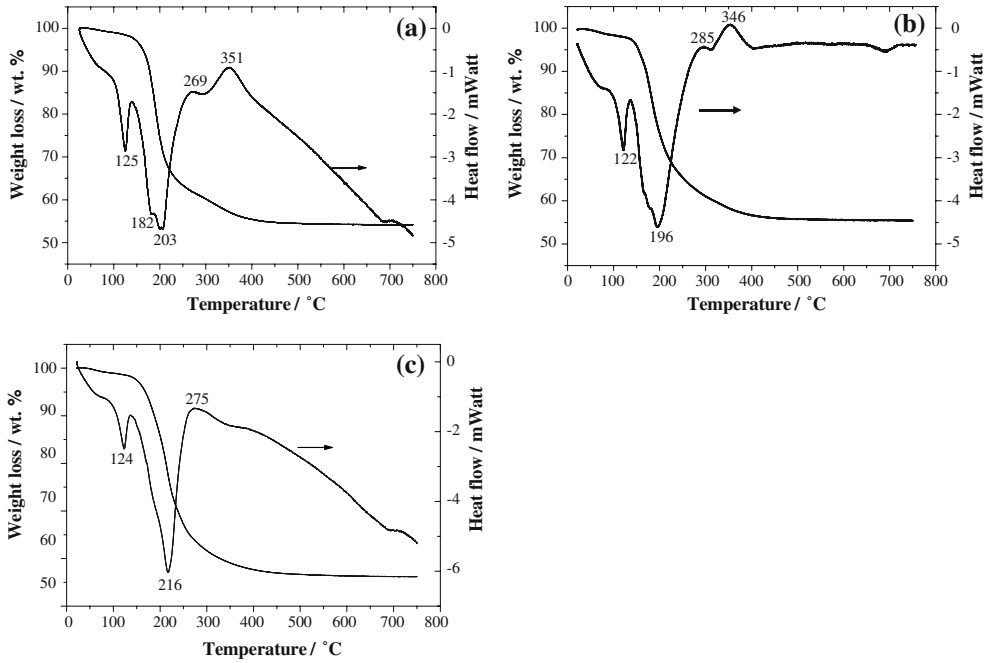

Figure 1. Thermogravimetric analysis and differential scanning calorimetric of the γ-Al_2O_3-supported Co(Ni)–Mo(W) catalyst precursors. 2.5 wt% CoO-12 wt% MoO_3/γ-Al_2O_3 (a), 3 wt% NiO-12 wt% MoO_3/γ-Al_2O_3 (b), 3 wt% NiO-19 wt% WO_3/γ-Al_2O_3.

A well-defined endothermic process centered at 125 °C and a broad stage involving at least two steps at 182 and 203 °C are observed. The first step attributed to the melting process of urea appears at lower temperature than melting point of urea (i.e., 135 °C [20]), probably due to the presence of ionic species within urea crystal structure that decreasing its melting temperature (colligative property). The broad band on the other hand is associated with the partial dehydration–decomposition of the Co and Mo precursor salts. Two exothermic processes at 269 °C and 351 °C are also displayed. The former stage is assigned to the urea combustion and total decomposition of the partially dehydrated Co and Mo precursors to produce the catalyst oxidic precursor. The latter is associated with a further combustion of residual organic matrix.

The TGA–DSC profiles of the alumina-supported 3% NiO-12% MoO_3 catalyst precursor are given in Figure 1B. The thermogram presents two major steps at about 85 °C and 182 °C with a total weight loss of 45.5 wt% in fairly good agreement with the expected value. The DSC profile, on the other hand, shows a similar behavior than that of Co–Mo catalyst precursor. Two endothermic processes at 122 °C and 196 °C associated with the melting process of urea and the partial dehydration–decomposition of the Ni and Mo precursor salts, respectively. The exothermic reaction at 285 °C is attributed to the urea combustion and total decomposition of the partially dehydrated Ni and Mo whereas the process at 346 °C is due to further combustion of residual organic matrix.

The TGA–DSC profile of the alumina-supported 3% NiO-19% WO_3 catalyst precursor is shown in Figure 1C. The thermogram displays two weight losses of 1.2 and 42.7 wt% at about 75 and 214 °C, respectively with a total weight loss of 43.9% in fairly good agreement with the theoretical value (i.e., 46.3 wt%). The DSC profile, on the other hand, shows two well-defined endothermic stages at 124 and ca. 216 °C owing to the urea melting and partial decomposition of urea and the precursor salts, respectively. Two weak exothermic processes at about 275 and ca. 384 °C are representative of a smooth combustion process. This indicates, in line with the thermal behavior of Co(Ni)–Mo catalysts, that the partial thermal decomposition overlapped the combustion reaction because of an overstoichiometric excess of urea. When part of urea is removed by a drying process (UMxD-prepared precursor) the stage attributed to the urea melting is not observed however the feature associated with the combustion process was clearly noted. This finding illustrates the influence of urea excess on the combustion process [12,21].

Several consecutive stages such as melting, dissolution and chemical reactions take place before and upon combustion process to transform the urea and the Co(Ni) and Mo(W) precursor salts to oxidic species over alumina surface. When the urea is melted, this is spread out over alumina surface and the Co (or Ni) and Mo (or W) salts are partially dissolved and dehydrated, a further increase of the temperature produces a partial decomposition both of the precursor salts and of the fuel. When the sample achieves the ignition temperature (ca. 200 °C), an exothermic reaction takes place. This releases heat and different gaseous molecules as a consequence of the total transformation of urea and the metal precursor salts.

The nature of combustion differs from flaming to non-flaming (smouldering) and also from the final product characteristics and its microstructure [15,22]. For the preparation of Al_2O_3-supported oxides this temperature is likely lowered not only by the stoichiometric excess of urea, but also the lower content of the Co (or Ni) and Mo (or W) precursor salts and the combustion-heat dissipation through the support. Considering these factors and the low alumina reactivity under combustion condition [23], it is thought that the transformation of the precursor salts proceeds under a reaction of solid state combustion. Even though, the UMxC-prepared oxidic precursors was obtained from a combustion process at the ignition temperature of 500 °C instead of a temperature-programed combustion, one can envisage that in a very short period of time (ca. 30 s) the sample undergoes water-removal and melting of urea followed by the combustion reaction to produce the oxidic catalyst precursor as was earlier mentioned.

3.1.2. Laser Raman spectroscopy

The Raman spectrum of the alumina-supported 2.5 % CoO-12% MoO_3 oxidic precursor displayed a dominant asymmetric band at 948 cm^{-1} and a small one at 344 cm^{-1}, attributed to the symmetric stretching and bending mode of the terminal Mo = O bond of octahedrally coordinated Mo species for hydrated $Mo_7O_{24}^{6-}$ anion, respectively (Figure 2a). In addition, the shoulder at 850 and the Raman bands at 556 and 222 cm^{-1} are associated with the asymmetric, symmetric and deformation modes of the Mo–O–Mo bridges for the polymolybdate species [24], respectively. A similar Raman spectrum shows the alumina-supported 3 % NiO-12% MoO_3 oxidic precursor (see Figure 2b). On the other hand, the Raman spectra of the alumina-supported 3% NiO-19% WO_3 precursor shows a small feature at 880 and a strong peak at 968 cm^{-1} ascribed to the symmetric stretchings of O–W–O polymeric linkages and W = O terminal of octahedrally-coordinated WO_6 units present in hydrated polytungstate structures, respectively (Figure 2c). Furthermore, a small Raman band at 368 cm^{-1} is associated with local WO_6 units [25]. Raman peaks attributed to Mo(or W)O_3 or Co(or Ni)O are not observed, suggesting that the UMxC synthesis favor the formation of well-dispersed oxidic species in line with the XRD results for low promoter loading-containing catalyst precursors (results no shown).

The Raman spectrum of the sulfurized alumina-supported 2.5Co–12Mo catalyst is rather similar to that of bulk 2H–MoS_2 [26], figure 3a. This shows major peaks at 381 and 405 cm^{-1}, which are assigned to the Mo–S stretching mode (E^1_{2g}) along the basal plane and the S–Mo–S bond mode along the c-axis or perpendicular to the basal plane (A_{1g}), respectively [27,28]. The Raman peaks characteristics of Mo–oxo species were not detected. Nevertheless, the Raman spectrum displayed poor peak intensity, most likely due to its coverage with residual carbon. Indeed, both a strong peak at 1595 and a broad band around 1355 cm^{-1} characteristics of residual carbon material were also observed [14].

On the other hand, the Raman spectrum for the sulfurized alumina-supported 3Ni–12Mo catalyst reveals two weak Raman features at ca. 369 and 397 cm^{-1}, Figure 3b. They are attributed to strongly distorted-MoS_2 along the basal plane since the Mo–S stretching mode (E^1_{2g}) along the basal plane and the S–Mo–S bond mode along the c-axis (A_{1g}) is observed at 381 and 405 cm^{-1} for a well-ordered MoS_2 structure [12]. The Raman spectrum of the sulfurized alumina-supported 3Ni–19W catalyst is displayed in Figure 3c. This sample shows very weak Raman peak intensity and no features related with W–oxo species, suggesting that the temperature employed was sufficient to obtain total

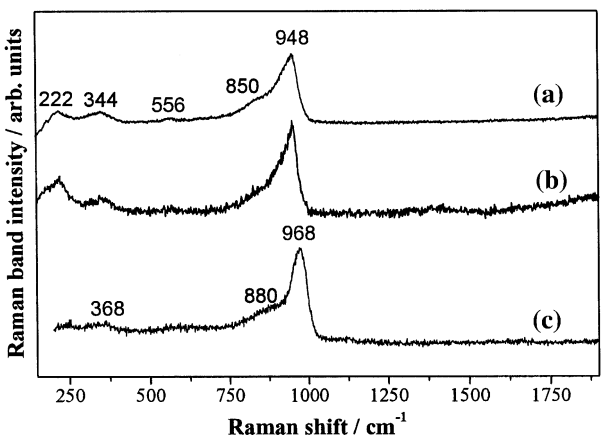

Figure 2. Laser Raman spectra of the γ-Al_2O_3-supported 2.5Co–12MoS_2 (a), 3Ni–12MoS_2 (b) and 3Ni–19WS_2 (c) HDS catalyst precursors.

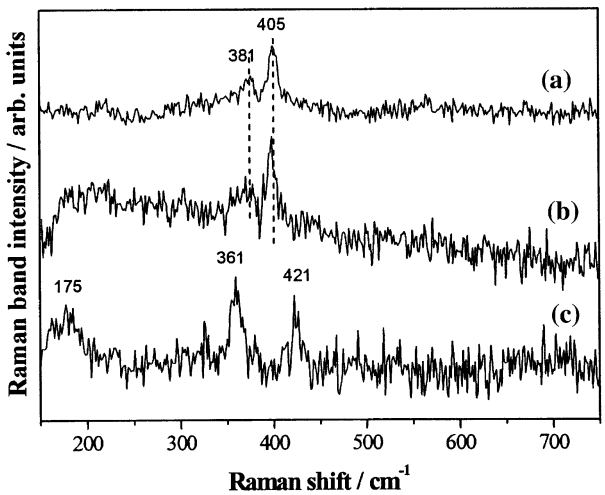

Figure 3. Raman spectra of the γ-Al_2O_3-supported bimetallic HDS catalysts using thiophene as sulfurizing agent. 2.5Co–12MoS_2/γ-Al_2O_3 (a), 3Ni–12MoS_2/γ-Al_2O_3 (b), 3Ni–19WS_2/γ-Al_2O_3 (c).

sulfurization [29]. The main observed features are characteristic of a MoS_2-type structure (i.e. 2H–WS_2). Two major first order peaks at 361 and 421 cm^{-1} and a weak broad band at 175 cm^{-1} are observed. The first feature is assigned to the W–S stretching mode (E^1_{2g}) along the basal plane, the second one corresponds to the S-W–S bond mode along the c-axis or perpendicular to the basal plane (A_{1g}) and the latter is attributed to second order Raman peaks [30,31]. The close correspondence between the Raman shift of the observed peaks and the data reported in the literature for single phase WS_2 [31] suggests the presence of a not strongly distorted tungsten sulfide structure. Since thiophene was employed as sulfurizing agent residual graphitic carbon was also observed. However the carbon content (0.2–0.5 wt%) was significantly lower than that of their Ni–Mo counterparts (1.0–2.1 wt%).

3.1.3. High resolution transmission electron microscopy

Representative HRTEM images of alumina-supported 2.5Co–12Mo and 3Ni–12Mo catalysts are shown in Figure 4. The micrographs display mainly the edge or prism planes oriented along or roughly parallel to the electron beam direction with layer stacking spacing of ca. 6 Å characteristic of bulky MoS_2, in line with the XRD patterns (results not shown). However, other orientations such as the basal planes and the (110) orientation were also observed but in less extent. In addition, dislocations where the slabs are partially intercalated by another slab and bent on a longer scale to maximize the interaction with the surface are also observed, see image 4b. On the other hand, the degree of stacking is around 3–4 layer and the slab length distribution are fairly broad with an average slab length of ca. 3 nm, owing to the relatively high sulfurizing temperature (i.e., 450 °C). Both images are quite similar to the Co-promoted MoS_2/γ-Al_2O_3 HDS catalysts prepared by impregnation and also sulfurizing with thiophene [12].

3.2. Determination of the optimal Co(Ni)/Mo(W) molar ratio for the HDS reaction

The dependence of the synergistic effect (SE) and the $C_4/C_4^=$ mole ratio upon the Ni or Co molar fraction [Co (or Ni)/ Co (or Ni) + Mo (or W)] is shown in Figure 5. The SE was evaluated according to:

$$SE = \frac{k_{\mathrm{Co(Ni)-Mo(W)}}}{[(\text{wt\% promoter/wt\% maximum loading of promoter})k_{\mathrm{Co(Ni)}} + k_{\mathrm{Mo(W)}}]}$$

where $k_{\mathrm{Co(Ni)}}, k_{\mathrm{Mo(W)}}$ and $k_{\mathrm{Co(Ni)-Mo(W)}}$ are pseudo first-order rate constants of the Ni (or Co) and Mo (or W) monometallic catalysts and the corresponding bimetallic Co(Ni)–Mo(W) catalysts. For monometallic catalysts $k_{\mathrm{Co(Ni)-Mo(W)}} = k_{\mathrm{Co(Ni)}}$ or $k_{\mathrm{Mo(W)}}$, depending on the catalyst compositions. This ratio equals unity if no synergism occurs and is higher than unity when a synergism effect is present.

The Co and Ni-promoted Mo catalysts showed not only thiophene conversions 3–5 times greater than the unpromoted Mo sample, but also a good catalytic stability during time on stream. The changes of the SE against the Co(Ni)/[Co(Ni) + Mo] mole ratios show a strong increases of the SE with rising promoter loadings. This achieved a maximum for Co molar fraction of 0.29 (molar Co/Mo ratio of 0.41) and 0.33 (molar Ni/Mo ratio of 0.49) for Ni molar composition and then decreased at higher promoter content, Figure 5A,

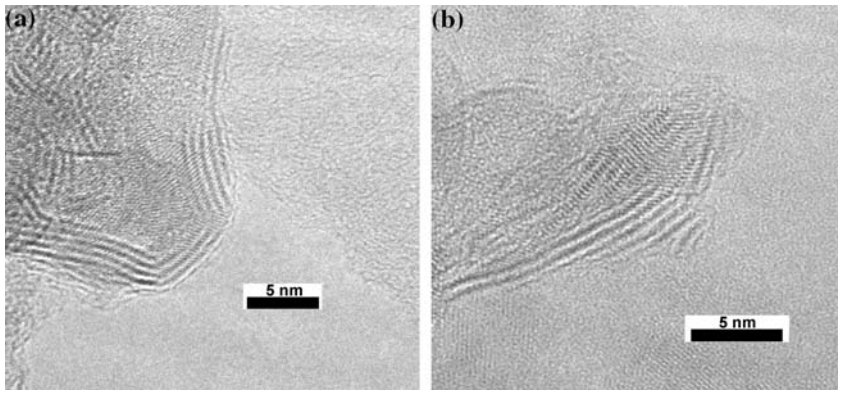

Figure 4. HRTEM images of the γ-Al_2O_3-supported bimetallic HDS catalysts using thiophene as sulfurizing agent. 2.5Co–12MoS_2/γ-Al_2O_3 (a), 3Ni–12MoS_2/γ-Al_2O_3 (b).

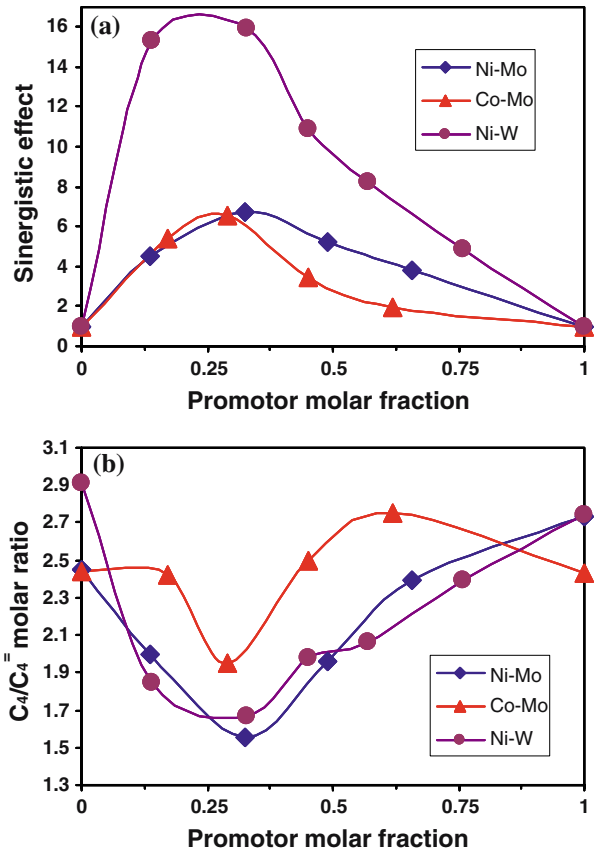

Figure 5. Dependence of the synergistic effect (SE) (a) and the $C_4/C_4^=$ molar ratio (b) on the γ-Al_2O_3-supported HDS catalyst compositions. Reactions conducted at 350 °C, 0.1 MPa and 100 mL(g_{cat}.min)$^{-1}$. Relative error for $C_4/C_4^=$ is ca. 5%.

probably due to the segregation of Co(or Ni)S_x. At promoter loadings above the optimal compositions, Ni–Mo catalysts showed clearly higher SE than alumina-supported Co–Mo catalysts. On the other hand, the dependence of the SE upon the Ni molar fraction for Ni–W HDS catalysts showed a similar behavior that the Co(Ni)–Mo catalysts described above, Figure 5A. However, the alumina-supported Ni-promoted WS_2 catalysts showed clearly higher synergistic effect into the studied composition range. Furthermore, the optimal SE, at Ni molar fraction of ca. 0.30 (molar Ni/W ratio of 0.43), was 2.5 times higher than those for Co(or Ni)-promoted Mo HDS catalysts. This finding is attributed to the relatively low HDS activities of the W- or Ni-containing monometallic catalysts compared with the Mo or Co(Ni) monometallic counterparts. Hence, the results suggest that the SE arises from the formation of a more active phase than that presents in the monometallic catalysts and also that the rise in the catalytic activity is likely due to the increase in the number of the active sites.

The dependence of the $C_4/C_4^=$ molar ratios on the promoter molar fraction is illustrated in Figure 5B. An opposite behavior relative to the SE is noted, which resulted more pronounced for Ni-containing catalysts. In fact, at approximately isoconversion (i.e., 60%) the relative rate of HYD to HDS for Ni/(Ni + W) of 0.14 (1Ni–19W) is just 10% above 3Ni–19W/Al_2O_3 catalyst (Ni molar fraction of 0.33). For alumina-supported Ni–Mo HDS catalysts under isoconversion condition (i.e., 50%), the relative rate for Ni/(Ni + Mo) of 0.14 (1Ni–12Mo) varied 20% compared with 12Ni–12Mo catalyst (Ni molar fraction of 0.66). This indicates that a slight antagonistic effect on the $C_4/C_4^=$ mole ratio is present in the thiophene HDS reaction carried out at atmospheric pressure. Therefore, synergistic effect increases markedly the C–S bond cleavage reaction whereas a less pronounced antagonistic effect affects the relative rate of hydrogen transfer reactions. Furthermore, under isoconversion (i.e., 64–66%) and maximum SE, alumina-supported 2.5Co–12Mo catalyst presented the highest trend toward the hydrogen transfer reactions.

The qualitative behavior of the SE curves for the γ-Al_2O_3-supported Co (or Ni)-Mo catalysts were similar to the earlier reports however the SE magnitudes and even the optimal catalyst composition were significantly different [32–34], owing to its strong dependence on the preparation method and the operation conditions [32]. For instance, the optimal composition and the qualitative behavior of the promoter effect of nickel on Mo-based HDS catalyst are rather similar to the earlier reports of Al_2O_3-supported Ni–Mo catalysts [33,34]. However, the optimal promoter effect (i.e., k_{Ni-Mo}/k_{Mo}) of the combustion-prepared catalyst was slightly lower (ca. 15%) than that recently given by Zdražil over impregnation-prepared Ni–Mo catalyst [35]. This is probably due to the coverage of the most active HDS sites by deposition of graphitic carbon upon sulfurizing process when thiophene is employed as a sulfurizing agent and/or the lateral growing of MoS_2 by sintering.

It is worth remarking that the optimal catalyst composition to reach a maximum HDS activity (i.e., Ni/W ~0.43) was significantly lower than those normally reported (i.e., Ni/W ~0.6–1.5) [29,33,36,37] and close to the recently given by Zuo *et al.* [38]. The higher Ni/W ratio necessary to obtain a maximum in activity for Al_2O_3-supported catalysts was explained by the sulfidation sequence of W and Ni. That is, Ni was sulfurized first forming bulk Ni sulfide but as soon as WS_2 slabs were formed Ni sulfide re-dispersed and even migrated to these slabs to form a CoMoS-type structure (NiWS) [39]. Since it is expected that not all bulk Ni sulfide will re-disperse and migrate to the WS_2 slabs a higher Ni loading to realize optimal NiWS formation was required [36]. However, for the catalyst series prepared by UMxC synthesis the optimal ratio was 0.43, which is indeed very close to the optimal theoretical ratio of 0.5, assuming that nickel is located at the edge plane of a perfect hexagonal structure of WS_2 with equal amounts of sulfur- and molybdenum-edge planes [32]. This fact

suggests that UMxC synthesis is a very efficient new approach to optimize the interaction between the supported oxidic precursors and therefore the HDS activity. In fact, we have obtained an optimal promoter effect (i.e., k_{Ni-W}/k_W) of 19, employing thiophene as sulfurizing agent, which is clearly greater than that usually found when H_2S is the sulfurizing agent (i.e. ca. 15) [29,36].

3.3. Influence of the sulfurization conditions over HDS catalytic performance

In order to study the effect of the sulfurizing agents on the optimal compositions of alumina-supported Ni–W and Ni–Mo HDS catalysts the influence of thiophene or H_2S in H_2 over the activity and $C_4/C_4^=$ molar ratio is shown in Figure 6. The catalysts exhibit very high catalytic stability during time on stream. It is noticeable that the H_2S-activated 3Ni–19W catalyst is markedly more active than C_4H_4S-activated counterpart and the 3Ni–12Mo catalysts, Figure 6A. Taking into account this fact, the activity trend can be rationalized considering a blocking effect of graphitic carbon on the active sites of C_4H_4 S-activated catalysts and a sintering process on H_2S-activated 3Ni–12Mo catalyst as the main causes of their lower HDS activity. Indeed, the optimal sulfurization temperature for Mo-based HDS catalysts using H_2S in H_2 as sulfuring agent is about 400 °C and above temperatures lead to a decrease of the HDS activity mainly due to lateral growing of MoS_2 and therefore descent of the edge active sites [32]. On the other hand, the sulfurizing agents also affect the relative rates of HYD to HDS reactions (i.e., $C_4/C_4^=$ molar ratio), see Figure 6B. The H_2 S-activated 3Ni–12Mo catalyst showed higher $C_4/C_4^=$ molar ratio than H_2 S-activated 3Ni–19W catalyst because of different thiophene conversions. However under isoconversion (ca. 65%) the H_2S-activated 3Ni–12Mo catalyst showed higher $C_4/C_4^=$ molar ratio than C_4H_4 S-activated catalysts, suggesting that the deposition of carbon markedly hinders the rates of hydrogen transfer reactions.

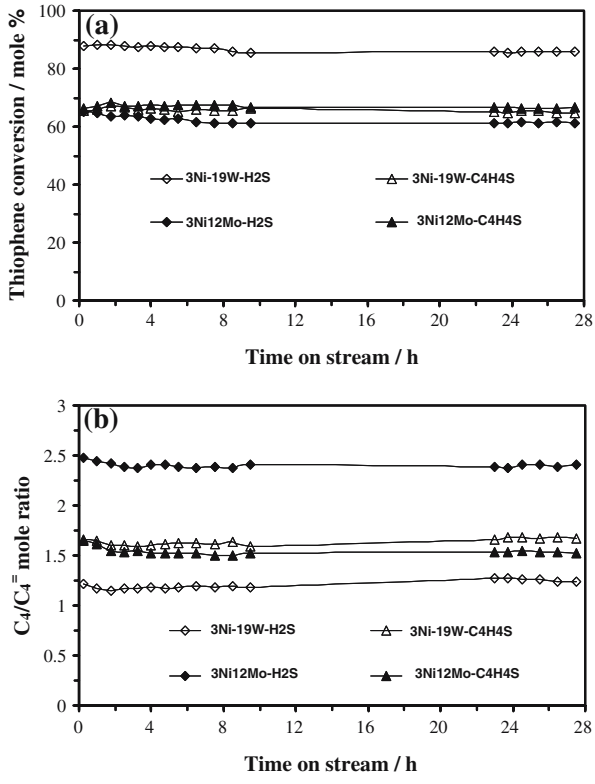

Figure 6. Catalytic behavior of alumina-supported 3Ni–19W(or 12Mo) treated with different sulfurizing agents at 450 °C. Reactions carried out at 350 °C, 0.1 MPa and 100 mL(g_{cat}.min)$^{-1}$.

To find out the effect of the sulfurizing temperatures over the catalytic behavior of alumina-supported 2.5Co–12Mo, 3Ni–12Mo and 3Ni–19W catalysts, the samples were sulfurized using 10% H_2S–H_2 to 400 or 450 °C. The HDS catalytic performance is summarized in Table 1. Regardless of the sulfurizing temperatures, the following activity order was obtained: 2.5Co–12Mo > 3Ni–19W > 3Ni–12Mo. The sulfurizing temperature showed a strong inhibition effect on the overall rate of 3Ni–12Mo catalyst, whereas slight variations in the activities of 2.5Co–12Mo and 3Ni–19W were observed. On the other hand, the $C_4/C_4^=$ molar ratios for the Mo-containing catalysts were clearly increased when rising sulfurizing temperatures, while for 3Ni–19W catalyst the relative rates of HYD to HDS reactions did not vary. For alumina-supported 2.5Co–12Mo catalyst the sulfurizing temperature markedly affects the hydrogen transfer reactions rather than the thiophene hydrodesulfurization rate in contrast with 3Ni–12Mo. This behavior is probably associated with the difference in MoS_2-edge preference between nickel and cobalt [40]. Which might affect the thermal stability of the Co(or Ni)MoS phases and hence their ability for hydrogen transfer reactions and/or C–S bond scission reactions. Furthermore, differences in the morphology of the active phase owing to the effect of the sulfurizing temperatures can also lead to large changes in the HDS catalytic behavior [41]. The above-mentioned trend contrasts with the poor influence of the sulfurizing

Table 1
Effect of the sulfurizing temperatures over the HDS catalytic performance

Catalyst[a]	H_2S-activated catalysts at 400 °C		H_2S-activated catalysts at 450 °C	
	[b]Overall rate	$C_4/C_4^=$	[b]Overall rate	$C_4/C_4^=$
2.5Co–12Mo	126	1.2	123	2.0
3Ni–19W	106	1.2	114	1.2
3Ni–12Mo	95	1.9	81	2.4

[a]Catalysts supported on γ-Al_2O_3.
[b]Reactions conducted at 350 °C, 0.1 MPa and 100 mL(g_{cat}.min)$^{-1}$, unit of HDS rate: (thiophene μmol/cat-g.min).

temperature on the HDS performance of alumina-supported 3Ni–19W catalyst. This is indicative of a low interaction between W–oxo species and alumina and/or a very efficient interaction among the well-dispersed oxidic precursors on the support surface that significantly facilitates the sulfurization process of W–oxo entities [37,38] and attenuates the influence of the sulfurizing temperature on the HDS catalytic performance.

The apparent activation energies and the pre-exponential factors derived from Arrehenius plot for the different catalysts are presented in table 2. Both kinetic parameters were determined in the temperature range of 250–325 °C. The apparent activation energies compare well with the data reported by Ledoux *et al*. [42] for thiophene-HDS reaction on carbon-supported metal sulfide clusters, which range from 69 to 98 kJ/mol. Furthermore, these values correspond with results of quantum chemical calculations obtained by Neurock and van Santen [43], suggesting that both C–S bond cleavage reactions and sulfur removal are potential rate limiting steps for thiophene HDS reaction. Nevertheless, the greatest apparent activation energies and pre-exponential factors for alumina-supported 2.5Co–12Mo and 3Ni–19W catalysts lead us to propose that the C–S bond scission reaction rather than hydrogenative sulfur removal is rate-limiting step. Since the highest pre-exponential factors suggest that a faster rate of sulfur removal via H_2S (i.e., desorption reaction) might play an important role for regenerating sulfur vacancies and leads to a large gain in entropy as compared to surface reactions [44]. On the other hand, the lower apparent activation energy for alumina-supported 3Ni–12Mo is similar to that determined by Hensen *et al*. [45] for Mo/C HDS catalyst (i.e., 66 kJ/mol), which was associated with H_2 activation reaction as rate-limiting step. One can tentatively propose that the relatively low pre-exponential factor for 3Ni–12Mo is therefore attributed to the adsorption of hydrogen from the gas phase, which leads to loss in entropy. However, differences in the number of sulfur vacancies or active site densities can also lead to large changes in the pre-exponential factor.

Table 2
Apparent activation energies and pre-exponential factors for γ-Al_2O_3-supported Co (or Ni)- Mo (or W) HDS catalysts

Catalyst Composition[a]	[b]$E_a^{(app)}$(kJ/mol)	[c]A_{pre}
2.5Co–12Mo	93 ± 1	1.54×10^9
3Ni–19W	85 ± 2	1.73×10^8
3Ni–12Mo	64 ± 3	2.15×10^6

[a]Catalysts supported on γ-Al_2O_3 and sulfurized under 10% H_2S–H_2 up to 400 °C.
[b]Apparent activation energy determined in the temperature range of 250-325 °C.
[c]Unit of pre-exponential factor: (thiophene mol/metal mol.h).

According to Hensen *et al*. [45], a high HDS activity is linked to a low thiophene reaction order, high apparent activation energy and high pre-exponential factor because of a strong thiophene-active phase interaction. Here, we extend that trend considering the fact that under thiophene isoconversion (ca. 10%) the following $C_4/C_4^=$ molar ratio was obtained: 5.4 (3Ni–12Mo) > 4.5 (3Ni–19W) > 3.4 (2.5Co–12Mo). This suggests that the hydrogen transfer reactions become more important when both the apparent activation energies and the pre-exponential factors are decreased, likely due to a strong hydrogen-active phase interaction or a poor competitive effect of H_2S for the H_2 adsorption sites. Indeed, the yield of the partially hydrogenated thiophenes (i.e., 2,3-dihydrothiophene, 2,5-dihydrothiophene and tetrahydrothiophene) produced during the hydrodesulfurization of thiophene on Mo/C and Co–Mo/C catalysts [46] showed a similar kinetic parameter trend than that for alumina-supported Co(Ni)–Mo(W) HDS catalysts. This indicates that the observed behavior is independent of the employed supports and also suggests that this trend seem to be universal for HDS catalysts.

It is worth pointing out that the apparent activation energies decreased ca. 25% for alumina-supported 2.5Co–12Mo and 3Ni–19W catalysts and only 12% for 3Ni–12Mo at temperatures above 350 °C. The pre-exponential factors on the other hand underwent a reduction of ca. 18% for 2.5Co–12Mo and 3Ni–19W catalysts and only 9% for 3Ni–12Mo catalyst. This behavior is not ascribed to mass-transfer limitations since experiments with different catalysts particles sizes revealed that these limitations are absent. This result has been attributed to the changes in the rate-limiting step in the HDS reaction mechanism [47] and/or to a decrease of reactant surface coverage as temperature increases [45,46]. The relationship between the apparent activation energy (E_a^{app}), when the reaction rate constant k has an Arrehenius-type behavior, and the real activation barrier of the rate-limiting step (E_a^{rls}) is the following:

$$E_a^{app} = E_a^{rls} + \left(1 - \Theta_T^{\#}\right) \cdot {}^{T}_{ads} + \left(1 - \Theta_H^{\#}\right) \cdot \Delta H_{ads}^{H_2} - \Theta_{H_2S}^{\#} \cdot \Delta H_{ads}^{H_2S}$$

where $\Theta H^{\#}$ and ΔH_{ads} are the surface coverage and the heat of adsorption of thiophene (T), hydrogen (H) and hydrogen sulfide (H_2S), respectively. When the reaction temperature is increased the surface coverage mainly of thiophene and H_2S decreased. This is reflected in a higher reduction both of the apparent activation energies and the pre-exponential factors for γ-Al_2O_3-supported 2.5Co–12Mo and 3Ni–19W catalysts, owing to the participation of S-containing molecules in the rate-limiting step. However the attenuation of the apparent activation energy was less severe for alumina-supported 3Ni–12Mo catalyst, because of a lower change of the

surface coverage when increasing reaction temperatures, which was also reflected in a smaller change in the pre-exponential factor.

4. Concluding remarks

The UMxC synthesis is a simple method for preparing supported catalysts in a short period of thermal treatment. Several consecutive stages such as urea melting, metal precursor dissolution and chemical reactions take place before and upon combustion process. The combustion reaction decomposes the urea and transforms the Co(Ni) and Mo(W) precursor salts to oxidic species over alumina surface.

The C_4H_4S/H_2-activated Co- (or Ni-) promoted MoS_2 (or WS_2) catalysts present a strong synergistic effect when the Co (or Ni)/Mo (or W) molar ratio is near to 0.5 whereas the $C_4/C_4^=$ molar ratios display a weak antagonistic effect, probably due to the deposition of carbon that markedly hinders the rates of hydrogen transfer reactions. The optimal SE for Ni–W catalyst was 2.5 times higher than those for Co (or Ni)-promoted Mo HDS catalysts. The sulfurizing temperature, employing 10% H_2S in H_2 as sulfurizing agent, significantly affects the HDS performance of alumina-supported Co(Ni)–Mo catalysts and in less extent the catalytic behavior of Ni–W catalysts, probably due to the efficient interaction among the supported oxidic precursors.

Based on the apparent activation energies and the pre-exponential factors the C–S bond cleavage reaction for alumina-supported Co(Ni)–Mo HDS catalysts is rate-limiting step for thiophene HDS reaction. For Ni-promoted WS_2 catalysts, on the other hand, the H_2 activation reaction rather than C–S bond cleavage reactions or sulfur removal seem to be rate-limiting step. The hydrogen transfer reactions become more important when both the apparent activation energies and the pre-exponential factors are decreased, likely due to a strong hydrogen-active phase interaction and/or a poor competitive effect of H_2S for the H_2 adsorption site.

Acknowledgments

S.L. González-Cortés is deeply indebted to the ULA and FONACIT (Venezuela) for financial support.

References

[1] EP directive 2003/17/EC, Official J. Eur. Union L 76, 46 (2003) 10.
[2] R. Prins, H.J. de Beer and G.A. Somorjai, Catal. Rev.-Sci. Eng. 31 (1989) 1.
[3] P.T. Vasudevan and J.L.G. Fierro, Catal. Rev.-Sci. Eng. 38 (1996) 161.
[4] R.R. Chianelli, M.H. Siadati, M. Perez De la Rosa, B. Gilles, P.W. Jess, B. Roby Jr. and L.A. Billie, Catal. Rev.-Sci. Eng. 48 (2006) 1.
[5] M. Sun, D. Nicosia and R. Prins, Catal. Today 86 (2003) 173.
[6] T. Shimizu, K. Hiroshima, T. Honma, T. Mochizuki and M. Yamada, Catal. Today 45 (1998) 271.
[7] J.A.R. van Veen, E. Gerkema, A.M. van der Kraan and A. Knoester, J. Chem. Soc., Chem. Commun. (1987) 1684.
[8] M. Zdražil, Catal. Today 3 (1988) 269.
[9] I. Bezverkhyy, P. Afanasiev, C. Geantet and M. Lacroix, J. Catal. 204 (2001) 495.
[10] N.A. Dhas, A. Ekhtiarzadeh and K.S Suslick, J. Am. Chem. Soc. 123 (2001) 8310.
[11] P. Pinto, M.J. Calhorda, T. Straub, V. Miikkulainen, J. Raty, M. Suvanto and T.A. Pakkanen, J. Mol. Catal. A: Chem. 170 (2001) 209.
[12] S.L. González-Cortés, T-C. Xiao, P.M.F.J. Costa, B. Fontal and M.L.H. Green, Appl. Catal. A: Gen. 270 (2004) 209.
[13] S.L. González-Cortés, T-C. Xiao, S.M.A. Rodulfo-Baechler and M.L.H. Green, J. Molec. Catal. A: Chem. 240 (2005) 214.
[14] S.L. González-Cortés, T-C. Xiao, T-W Lin and M.L.H. Green, Appl. Catal. A: Gen. 302 (2006) 264.
[15] K.C. Patil, S.T. Aruna and T. Mimani, Curr. Opin. Solid State Mater. Sci. 6 (2002) 507.
[16] G. Xanthopoulou and G. Vekinis, Appl. Catal. B: Environ. 19 (1998) 37.
[17] J.B. Peri, J. Phys. Chem. 69 (1965) 211.
[18] J.H. DeBoer, J.M.H. Fortuin, B.C. Lippens and W.H. Meijs, J. Catal. 2 (1963) 1.
[19] H. Knözinger and P. Ratnasamy, Catal. Rev.-Sci. Eng. 17 (1978) 31.
[20] R.C. Weast and M.J. Astle, eds., *CRC Handbook of Chemistry and Physics* 61 ed. (CRC Press Boca Raton, 1980).
[21] S.L. González-Cortés, T-C. Xiao, and M.L.H. Green, accepted in Stud. Surf. Sci. Catal.
[22] K. Suresh and K.C. Patil, in *Perspective in: Solid State Chemistry*, (ed.) K.J. Rao (Narosa Publishing House, New Delhi, 1995), p. 376.
[23] J.J. Moore and H.J. Feng, Prog. Mater. Sci. 39 (1995) 275.
[24] G. Mestl and T.K.K. Srinivasan, Catal. Rev.-Sci. Eng. 40 (1998) 451.
[25] M.M. Ostromecki, L.J. Burchman, I.E. Wachs, N. Ramani and J.G. Ekerdt, J. Molec. Catal. 132 (1998) 43.
[26] J.M. Chen and C.S. Wang, Solid State Comm. 12 (1974) 857.
[27] J.L. Verble and T.J Wieting, Phys. Rev. Lett. 25 (1970) 362.
[28] T.J. Wieting and J.L Verble, Phys. Rev. B. 3 (1971) 4286.
[29] C-H. Kim, W.L. Yoon, I.C. Lee and S.I. Woo, Appl. Catal. A: Gen. 144 (1996) 159.
[30] T. Sekine, T. Nakashizu, K. Toyoda, K. Uchinokura and E. Matsuura, Solid State Comm. 35 (1980) 371.
[31] J.-W. Chung, Z.R. Dai and F.S. Ohuchi, J. Cryst. Growth 186 (1998) 137.
[32] H. Topsøe, B.S. Clausen and F.E. Massoth, in *Hydrotreating Catalysis, Science and Technology*, (eds.) J R. Anderson and M. Boudart (Springer-Verlag, Berlin, 1996).
[33] S.P Ahuja, M.L. Derrien and J.F. Le Page, Ind. Eng. Chem. Prod. Res. Develop. 9 (1970) 272.
[34] V.H.J. de Beer, T.H.M. van Sin Fiet, J.F. Engelen, A.C. van Haandel, M.W.J. Wolfs, C.H. Amberg and G.C.A. Schuit, J. Catal. 27 (1972) 357.
[35] M. Zdražil, Catal. Today 86 (2003) 151.
[36] M.J. Vissenberg, Y. van der Meer, E.J.M. Hensen, V.H.J. de Beer, A.M. van der Kraan, R.A. van Santen and J.A.R. van Veen, J. Catal. 198 (2001) 151.
[37] T. Kabe, W. Qian, A. Funato, Y. Okoshi and A. Ishihara, Phys. Chem. Chem. Phys. 1 (1999) 921.
[38] D. Zuo, M. Vrinat, H. Nie, F. Maugé, Y. Shi, M. Lacroix and D. Li, Catal. Today 93–95 (2004) 751.
[39] H.R. Reinhoudt, Y. van der Meer, A.M. van der Kraan, A.D. van Langeveld and J.A. Moulijn, Fuel Process. Technol. 61 (1999) 43.
[40] M. Sun, A.E. Nelson and J. Adjaye, J. Catal. 226 (2004) 32.

[41] E.J.M. Hensen, P.J. Kooyman, Y. van der Meer, A.M. van der Kraan, V.H.J. de Beer, J.A.R. van Veen and R.A. van Santen, J. Catal. 199 (2001) 224.
[42] M.J. Ledoux, O. Michaux and G. Agostini, J. Catal. 102 (1986) 275.
[43] M. Neurock and R.A. van Santen, J. Am. Chem. Soc. 116 (1994) 4427.
[44] R.A. van Santen, M.J. Vissenberg, G. Vorbeck, P.W. de Bont, E. Boellaard, A.M. van dar Kraan and V.H. de Beer, Stud. Surf. Sci. Catal. 92 (1995) 221.
[45] E.J.M. Hensen, H.J.A. Brans, G.M.H.J. Lardinois, V.H.J. de Beer, J.A.R. van Veen and R.A. van Santen, J. Catal. 192 (2000) 98.
[46] E.J.M. Hensen, M.J. Vissenberg, V.H.J. de Beer, J.A.R. van Veen and R.A. van Santen, J. Catal. 163 (1996) 429.
[47] A.N. Startsev, Catal. Rev.-Sci. Eng. 37 (1995) 353.